

# Decentralized Collaborative Load Transport by Multiple Robots

Gustavo Montemayor and John T. Wen  
Department of Electrical, Computer, & Systems Eng.  
Rensselaer Polytechnic Institute  
Troy, NY 12180.  
Emails: {gustavo,wen}@cat.rpi.edu

**Abstract**—With the rapid progress of the robotic technology, it is becoming increasingly common to have multiple robots working together for material transport, cooperative assembly, etc. To ensure the proper handling of the load, especially if it is fragile or needs to be moved rapidly, the constraint force needs to be carefully managed. Tight force coordination is possible if all robots share their force information and the grasp geometry is completely known. When this is not the case, a common approach is to use the leader/follower strategy, where the leader provides the position control for the load and other robots comply based on the individual contact force measurements. This paper considers an alternate decentralized motion and force control method, where all robots participate in the control of the load *without* sharing any position and force information. Under centralized squeeze force control, robot motion is not affected. However, when the force control is decentralized, a perturbation term is added to the motion control loop. We show that the nominal exponential stability of the motion loop preserves the closed loop stability in the presence of this perturbation. Simulation and experimental results are included to demonstrate the proposed approach.

## I. INTRODUCTION

The use of a collection of robots to execute a common task such as material transport or cooperative assembly is becoming increasingly common as the costs of robotic hardware, processing power and software are reduced. Using multiple robots versus a single robot has the advantage of distributing a load among several smaller and less expensive robots, and tighter control of the internal force of the payload. In addition, there may be increased dexterity in handling the payload (such as in multi-finger manipulation), fault tolerance (defect of a subset of robots may not completely derail the task), and reconfigurability (the robots may be reconfigured to fit different distributed sensing and actuation needs). Collaborative transport of a load is also common in the biological world. Two ant species that are most proficient in group transporting, *Pheidologeton diversus* and *Oecophylla smaragdina*, form some of the largest perennial colonies [1]. Indeed, ants have served as the motivation of several mobile robot testbeds [2], [3].

There has been a considerable amount of research results related to the control of multiple robots handling a shared payload. A common assumption is that the geometry is completely known to all robots and the contact force mea-

surement is available. In this case, a passivity based motion control strategy combined with integral force control is proposed in [4]. An event-based control scheme is used in [5] where the internal force is regulated by modifying the desired trajectory at a supervisory level. In [6], [7] the payload dynamics (mass/inertia, location of center of mass) is used in the control law. Adaptive control version has been proposed in [8], [9].

The controllers described above perform well when all measurements and kinematics/dynamics information are available and centralized. However, as the number of robots increases, such schemes become impractical due to the corresponding increase in processing power and communication bandwidth requirements. Furthermore, the kinematics and dynamics information may not be fully available.

Another class of multi-robot control algorithm assumes that the geometry is precisely known but the contact forces are not measured. A leader broadcasts its estimated position and velocity and the followers simply try to keep up by using the known relative geometry [10]–[12]. There is no internal force control and the communication delay is not considered. When the grasp geometry is not known but the individual contact forces are measured, the most common approach is the leader/follower (also known as master/slave) scheme where the leader performs the position control and the followers simply comply [13]. In [14], the coordination of fixed-based manipulators is extended to the mobile base case. The mobile bases are treated as coarse/slow macro-motion and the manipulators as accurate fast mini-devices. In [15], [16], a similar leader/follower scheme for multiple mobile manipulators motivated by caster wheels is proposed.

This paper extends the centralized multi-robot motion and force control in [4] to the decentralized case. As a simple initial case to investigate, the robots are assumed rigidly attached to the load, and all robots and the load are in a plane. We also assume that there is no explicit communication of measured signals between the robots, so the controller structure is fully decentralized. We adopt the move/squeeze decomposition approach in [4] and address the motion loop first without considering the force and then study the force loop with motion induced force as a disturbance. For the decentralized motion control, we strengthen

the result in [4] to semi-global exponential stability. The decentralized force control adds a perturbation term to the motion loop. Due to the robustness inherent in exponential stability, the closed loop system remains stable. In the case that the desired motion of the load is from rest to rest, both motion and force converge to the desired setpoints exponentially. Simulation and experimental results are included to illustrate the approach. Due to the space limitation, we only state the stability results here. The complete proofs may be found in [17].

*Notation:* Given a matrix  $A$ ,  $\mathcal{R}(A)$  and  $\mathcal{N}(A)$  denote the range space and null space of  $A$ , respectively, and  $\tilde{A}$  denotes the full rank matrix such that  $\mathcal{N}(\tilde{A}) = \mathcal{R}(A)$ . In considering spatial quantities, we adopt the convention of placing the orientation variables (angular position, velocity and acceleration, and torque) before the translational variables (linear position, velocity, acceleration, and force).

## II. DYNAMICAL MODEL

Consider  $N$  multiple planar point robots rigidly holding a common load as shown in Figure 1. Note that rigid grasp means that the robots can push as well as pull without breaking contacts. The equation of motion is

$$\begin{aligned} m_i \ddot{x}_i &= F_i - f_i, \quad i = 1, \dots, N \\ M_c \ddot{x}_c &= \sum_{i=1}^N A_{ic}^T f_i \\ x_i &= \phi_i(x_c) \end{aligned} \quad (1)$$

where  $x_i \in SE(2)$  is the configuration of robot  $i$  which has the mass-inertia  $m_i$  and is subject to the applied spatial force  $F_i$  and exerts spatial force  $f_i$  to the load,  $x_c \in SE(2)$  is the configuration of a frame attached to the load which has the mass-inertia matrix  $M_c$  and  $\phi_i$  is the rigid body kinematic constraint:

$$\phi(x_c) = \begin{bmatrix} \theta \\ x_c^{(x)} - c_\theta r_{ic}^{(x)} + s_\theta r_{ic}^{(y)} \\ x_c^{(y)} - s_\theta r_{ic}^{(x)} - c_\theta r_{ic}^{(y)} \end{bmatrix}, \quad (2)$$

where  $\theta$  is the orientation of the load,  $s_\theta := \sin \theta$ ,  $c_\theta := \cos \theta$ ,  $(r_{ic}^{(x)}, r_{ic}^{(y)})$  and  $(x_c^{(x)}, x_c^{(y)})$  are the  $(x, y)$  components of  $r_{ic}$  in the inertial frame, respectively. Differentiating the constraint equation (2) once, we get the velocity constraint equation

$$\dot{x}_i = A_{ic} \dot{x}_c \quad (3)$$

where  $A_{ic}$  is the Jacobian from  $\dot{x}_c$  to  $\dot{x}_i$ :

$$A_{ic} = \begin{bmatrix} 1 & 0 & 0 \\ (s_\theta r_{ic}^{(x)} + c_\theta r_{ic}^{(y)}) & 1 & 0 \\ -c_\theta r_{ic}^{(x)} + s_\theta r_{ic}^{(y)} & 0 & 1 \end{bmatrix}. \quad (4)$$

Differentiating once more, we get the acceleration constraint equation:

$$\dot{x}_i = A_{ic} \ddot{x}_c + \dot{A}_{ic} \dot{x}_c \quad (5)$$

where

$$\dot{A}_{ic} = \begin{bmatrix} 0 & 0 & 0 \\ c_\theta r_{ic}^{(x)} - s_\theta r_{ic}^{(y)} & 0 & 0 \\ s_\theta r_{ic}^{(x)} + c_\theta r_{ic}^{(y)} & 0 & 0 \end{bmatrix}. \quad (6)$$

The equation of motion can be more compact written as

$$\begin{aligned} M \ddot{x} &= F - f \\ M_c \ddot{x}_c &= A^T f \\ x &= \phi(x_c), \quad \dot{x} = A \dot{x}_c, \quad \ddot{x} = A \ddot{x}_c + \dot{A} \dot{x}_c \end{aligned} \quad (7)$$

where  $M = \text{diag}\{m_1, \dots, m_N\}$ ,  $x$ ,  $\dot{x}$ ,  $\ddot{x}$ ,  $\phi$ ,  $F$ ,  $f$  are the stacked up version of  $x_i$ ,  $\dot{x}_i$ ,  $\ddot{x}_i$ ,  $\phi_i$ ,  $F_i$ , and  $f_i$ , respectively, and

$$A^T = [A_1^T, \dots, A_N^T]. \quad (8)$$

Note that the constraint equation  $x = \phi(x_c)$  may be written as

$$\underbrace{\begin{bmatrix} I \\ \vdots \\ I \end{bmatrix}}_{:=\mathcal{O}} x_c = \phi^{-1}(x). \quad (9)$$

Let  $\tilde{\mathcal{O}}$  be the full rank matrix such that  $\mathcal{N}(\tilde{\mathcal{O}}) = \mathcal{R}(\mathcal{O})$ . Then  $x$  satisfies the kinematic constraint if and only if

$$\tilde{\mathcal{O}} \phi^{-1}(x) = 0. \quad (10)$$

The objective of the control problem is to choose  $F$  so that  $(x_c, \dot{x}_c) \rightarrow (x_{c_{des}}, 0)$ , while regulating the force imparting on the load, e.g.,  $f$  maintained about a force setpoint  $f_{des}$ .

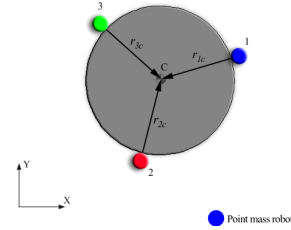


Fig. 1. Multiple point robots rigidly holding a load.

## III. DECENTRALIZED MOTION AND FORCE CONTROL LAW

For multiple articulated robots rigidly holding a rigid load, a motion/force control law has been proposed in [4] based on the so-called move/squeeze decomposition:

$$F = F_m + F_s \quad (11)$$

where  $F_m$  controls the motion and  $F_s$ , which is termed squeeze force control and chosen to satisfy

$$F_s \in \mathcal{N}(A^T), \quad (12)$$

controls the internal (squeeze) force of the payload. The motivation for this control law is based on the observation: *motion control affects force, but force control does not affect motion*. In other words, the motion and force loops are only one-way coupled. This leads to the design

strategy in [4]: the motion control is designed first without considering force, then force control is designed with motion induced force treated as a disturbance. However, the resulting control law is centralized. In this paper, we present a new decentralized implementation and show its closed loop stability.

#### A. Decentralized Motion Control

First consider the motion control. Define  $\Delta x_c = x_c - x_{c_{des}}$  and  $\Delta x = x - x_{des}$ , where  $x_{des}$  is chosen to be kinematically consistent with  $x_{c_{des}}$  (i.e.,  $\phi(x_{c_{des}}) = x_{des}$ ). By using the following energy-motivated Lyapunov function

$$V = \frac{1}{2}\dot{x}_c^T M_c \dot{x}_c + \frac{1}{2}\dot{x}^T M \dot{x} + \frac{1}{2}\Delta x^T K_p \Delta x, K_p > 0, \quad (13)$$

the proportion-derivative (PD) control law

$$F_m = -K_p \Delta x - K_d \dot{x}, \quad K_d > 0, \quad (14)$$

has been shown to be globally asymptotic stable in [4], but the steady state behavior has not been fully characterized. If  $K_p$  and  $K_d$  are chosen to be block diagonal (consisting of  $3 \times 3$  blocks), then the control law is fully decentralized in that each robot only needs to use its own position and velocity feedback as well as where its own desired position should be.

By adding a ‘‘cross term’’ in the energy Lyapunov function (13) (first used in [18] for serial, an open-chain robots), we can now strengthen this result. The proposition below characterizes the steady state structure, allows for both kinematically feasible and infeasible  $x_{des}$ , and shows that the convergence is exponential. We shall see later that the exponential stability property is important in ascertaining the stability under the decentralized motion and force control law as the motion and force loops become coupled.

*Proposition 1: Given the dynamical equation (7) and the control law (14), the following are true:*

- 1) *there exists a unique  $x^*$  that satisfies*

$$A^T K_p (x^* - x_{des}) = 0, \quad (15)$$

*that is globally asymptotically stable and semi-globally exponentially stable.*

- 2) *If  $\dot{A} = 0$ , then  $x^*$  is globally exponentially stable.*
- 3) *If  $x_{des}$  satisfies the kinematical constraint (10), then  $x^* = x_{des}$ .*

Note that though (14) is fully decentralized, the desired positions of the robots,  $x_{des_i}$ , are assumed to be synchronized. If this is not the case, i.e., there are relative time shifts between the desired positions, the transient performance will be affected, but not the steady state convergence. In the trajectory tracking case, this will result in a larger tracking error.

In Proposition 1,  $x_{des}$  may be chosen to be kinematically infeasible, i.e.,  $\tilde{\phi}^{-1}(x_{des}) \neq 0$ , and the robot configuration  $x$  still converges to a unique steady state. The result below shows that every vector in  $\mathcal{N}(A^T)$  corresponds to at least one  $x_{des}$ . This fact may be exploited to find the

contact geometry,  $A$  in (4), which is needed for choosing the force setpoint later.

*Proposition 2: Define  $g(x_{des}) := K_p(x^* - x_{des})$ , where  $x^*$  given by (15) in Proposition 1. Then  $\mathcal{R}(g(x_{des})) = \mathcal{N}(A^T)$ .*

#### B. Force Control

By eliminating  $\ddot{x}$  and  $\ddot{x}_c$ , we can solve for the contact force,  $f$ :

$$f = (MAM_c^{-1}A^T + I)^{-1}(F - M\dot{A}\dot{x}_c). \quad (16)$$

Decompose  $f$  as  $f = f_m + f_s$  where  $f_m \in \mathcal{R}(A)$  and  $f_s \in \mathcal{N}(A^T)$ . Note that this decomposition is not unique – it depends on the choice of units. The decomposition could also be viewed as a least square problem: Given  $f$ , find  $f_m$  to minimize  $\|f_m\|_W$  such that  $A^T f = A^T f_m$ , where  $\|\cdot\|_W$  is a weighted Euclidean norm with the weighting matrix  $W$ . Choosing units is then equivalent to selecting  $W$ .

Substitute the control law (11) into (16) and projecting on  $\mathcal{N}(A^T)$  we obtain

$$\begin{aligned} f_s &= F_s + \gamma \\ \gamma &:= -\tilde{A}^T(\tilde{A}\tilde{A}^T)^{-1}\tilde{A}(MAM_c^{-1}A^T + I)^{-1}MAM_c^{-1}A^T F_m \\ &\quad - (MAM_c^{-1}A^T + I)^{-1}M\dot{A}\dot{x}_c \end{aligned} \quad (17)$$

1) *Centralized Force Control:* In [4], the following linear squeeze force control law has been proposed:

$$F_s = -C(s)(f_s - f_{s_{des}}) + f_{s_{des}}, \quad (18)$$

where  $f_s = \tilde{A}^T(\tilde{A}\tilde{A}^T)^{-1}\tilde{A}$  ( $\tilde{A}$  is full row rank and  $\mathcal{N}(\tilde{A}) = \mathcal{R}(A)$ ) is the squeeze component of  $f$  and  $f_{s_{des}}$  is the specified squeeze setpoint. The controller  $C(s)$  is a scalar linear time invariant (LTI) filters operating on each component of  $f_s - f_{s_{des}}$ . The closed loop system is

$$(1 + C(s))\Delta f_s = \gamma, \quad \Delta f_s := f_s - f_{s_{des}}. \quad (19)$$

We should choose  $C(s)$  to have the following properties:

- 1) **Stability:**  $(1 + C(s))$  has all the zeros in the open left half plane.
- 2) **Zero steady state error:**  $C(s)$  should have at least a pole at the origin (integral control) to remove the steady state error.
- 3) **Disturbance rejection:**  $C(s)$  should have high gains over the spectrum of  $\bar{\gamma}$  to minimize the effect of motion on force control.
- 4) **Robustness:**  $C(s)$  should be chosen to have sufficient phase lead to ensure large phase margin which translates to good robustness property with respect to the force feedback time delay.

To implement the force control law (17), each robot needs the full contact force information in order to extract  $f_s$  from  $f$ . Because of this, the force control loop is inherently centralized. A common choice of  $C(s)$  that meets the stability, zero steady state error, and robustness requirements above is the integral force feedback,  $C(s) = \frac{k_f}{s}$ . To improve transient performance, it is also easy to incorporate gain adaptation, e.g., for the  $i$ th robot:

$$\dot{k}_{f_i} = -\alpha(k_{f_i} - k_{f_{i,nom}}) + \beta \|f_{s_i} - f_{s_{i,des}}\|^2.$$

2) *Decentralized Force Control*: We now consider the decentralized implementation of (18):

$$F_s = -C(s)(f - f_{s_{des}}) + f_{s_{des}}. \quad (20)$$

For simplicity, we shall consider integral force feedback only. Since the full spatial force is used in the feedback,  $F_s$  is no longer in  $\mathcal{N}(A^T)$ . Therefore, the motion and force loops are coupled. By using the new exponential stability result in Proposition 1, we show in the main result below that the coupled system is still globally stable.

*Theorem 1*: Given the dynamical equation (7) and the motion control law (14) and force control law (20) with  $C(s) = 1/s$ . Suppose  $M_c$  and  $A$  are both constant matrices. The following statements are true:

- 1) Motion and force,  $x$ ,  $\dot{x}$ , and  $f$ , are bounded for all  $t$ .
- 2) If  $\dot{x}(0) = 0$ , then  $(x, \dot{x}) \rightarrow (x^*, 0)$  and  $f_s \rightarrow f_{s_{des}}$  as  $t \rightarrow \infty$ , where  $x^*$  is the unique solution of (15).

The assumption  $M_c$  and  $A$  are constant basically restricts the motion to be pure translation. Allowing rotation means  $M_c$  and  $A$  may be time varying. The proof for this case is still under development.

The motion and force control law (14) and (20) are fully decentralized, i.e., each robot only uses its own motion and force error in the feedback. To generate the force setpoint  $f_{s_{des}}$  in  $\mathcal{N}(A^T)$  without the explicit knowledge of  $A$ , we can draw on Proposition 2. By choosing  $x_{des}$  to be deliberately kinematically infeasible and applying decentralized motion control (without force control), a basis for  $\mathcal{N}(A^T)$  may be generated from the steady state position error, which in turn can be used for choosing the direction of  $f_{s_{des}}$ .

### C. Simulation results

Consider three point robots holding a spherical load as shown in Figure 1. The simulation parameters are given in Table I (note that we have added linear viscous damping to the load,  $b_c$  for rotation and  $b$  for translation). The robots are located at (in the load frame)

$$r_{1c} = -R_c \begin{bmatrix} \cos(0.3) \\ \sin(0.3) \end{bmatrix}, \quad r_{2c} = -R_c \begin{bmatrix} \cos(0.3 + 2\pi/3) \\ \sin(0.3 + 2\pi/3) \end{bmatrix},$$

$$r_{3c} = -R_c \begin{bmatrix} \cos(0.3 - 2\pi/3) \\ \sin(0.3 - 2\pi/3) \end{bmatrix}.$$

The center of the load is initially at the origin with load frame aligned with the world frame.

$m_c$	1Kg
$I_c$	0.005 Kg-m <sup>2</sup>
$b_c$	2.5 N-m-s
$b$	0.5 N-m-s
$m_i$	1.5Kg
$R_c$	0.1 m

TABLE I  
SIMULATION PARAMETERS

By randomly generating an infeasible position setpoint  $x_d$ , as shown in Figure 2, the steady position error generates

a vector in  $\mathcal{N}(A^T)$  which can be in turn be scaled and used as the direction for the squeeze setpoint. The force setpoint that we use for all the subsequent simulation is

$$f_d = \begin{bmatrix} -20.92 & -6.51 & 16.12 & -14.93 & 4.89 & 21.35 \end{bmatrix}. \quad (21)$$

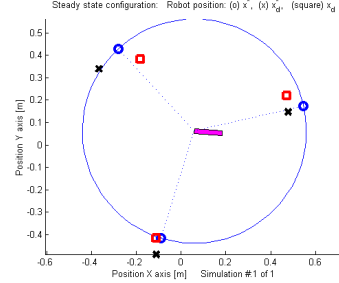


Fig. 2. A kinematically feasible desired position,  $x_d^*$  ( $\times$ ), is perturbed to a kinematically infeasible desired position,  $x_d$  ( $\square$ ). The robots converge to a steady state configuration,  $x^*$  ( $\circ$ ). The position error provides information on the squeeze subspace. The bar at the center of the load indicates the orientation.

As discussed in Proposition 2, by randomly choosing multiple kinematically infeasible  $x_d$ 's, we can use the steady state position error to estimate the complete squeeze subspace  $\mathcal{N}(A^T)$ . We illustrate this by randomly generating 45 infeasible setpoints and record the corresponding steady state errors,  $\Delta x_k := x_k^* - x_{k_{des}}$ . The non-zero singular values of  $\begin{bmatrix} \Delta x_1 & \dots & \Delta x_N \end{bmatrix}$  are plotted versus  $N$  in Figure 3. It can be seen that after 3 random moves, a basis of  $\mathcal{N}(A^T)$  is obtained (i.e., there are three non-zero singular values).

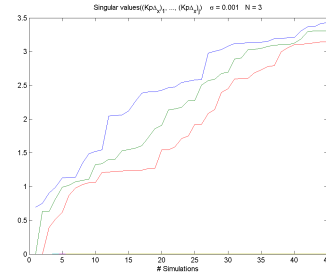


Fig. 3. Evolution of singular values of  $K_p[\Delta x_1, \dots, \Delta x_N]$  as a function of  $N$

We now consider the decentralized motion and force control with the load setpoint  $x_{c_d} = \begin{bmatrix} 0 \text{rad} & 0.3 \text{m} & 0.1 \text{m} \end{bmatrix}^T$  and the force setpoint (21). The desired motion trajectory is generated by using the trapezoidal velocity profile. The motion of the load is shown in Figure 4 with the corresponding trajectories in Figure 5. The contact forces in terms of the magnitude and angular deviation from the contact normal are shown in Figure 6. The transient phase of the motion produces some force disturbance, but the contact forces only deviate by a small amount from the contact normals. Therefore, for this case, the rigid grasp assumption is justified even under frictional contacts.

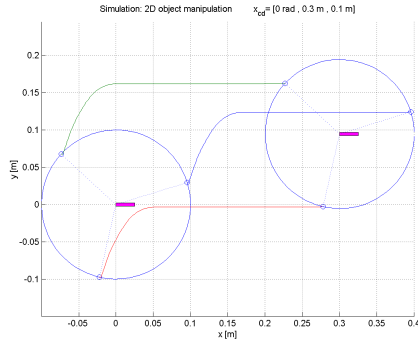


Fig. 4. Motion of load tracking a trapezoidal velocity profile

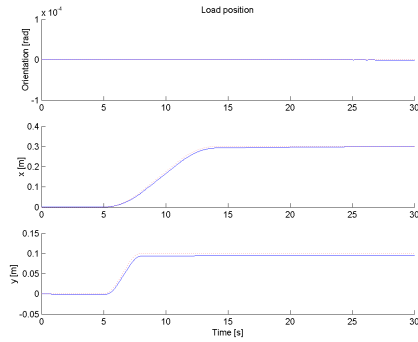


Fig. 5. Motion trajectory of load tracking a trapezoidal velocity profile

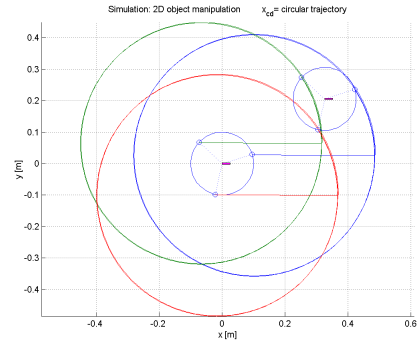


Fig. 7. Motion of load tracking a circular trajectory

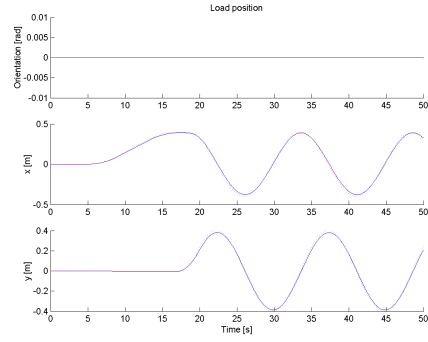


Fig. 8. Motion trajectory of load tracking a circular trajectory

Figure 7 shows the load tracking a circular trajectory. The trajectory of  $x_c$  is shown in Figure 8. Though the trajectory is followed closely, there is a large induced force transient as shown in Figure 9. However, since the squeeze force setpoint chosen sufficiently large, the angular deviations from the contact normals are still small (about 3 degrees).

When the desired motion trajectory is not synchronized (e.g., due to fixed delays between the individual clocks), the motion is still asymptotically stable, but there is a larger transient error, as shown in Figure 10. There is also a correspondingly larger force disturbance. In a continuous trajectory tracking case, the asynchronicity between robots

will cause a persistent tracking error as shown in Figures 11 and 12.

#### IV. EXPERIMENTAL RESULTS

The experimental testbed consists of two PUMA 560 robots each with a six-degrees of freedom Force/Torque sensor mounted on the wrist as shown in Figure 13. The control architecture is shown in Figure 14. Two DSP cards perform the real time control and data acquisition for the robots. The communication between the supervisory computer and the DSP, and between the two robot DSP controllers (not used for this paper), is through the Network Data Delivery Service (NDDS) middleware by Real Time

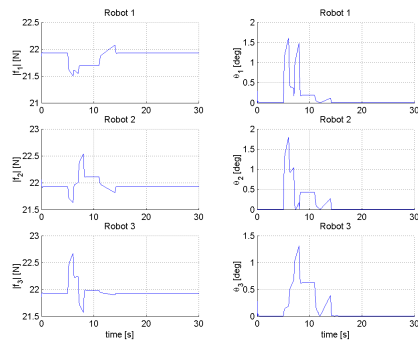


Fig. 6. Contact force trajectory while the load is tracking a trapezoidal velocity profile

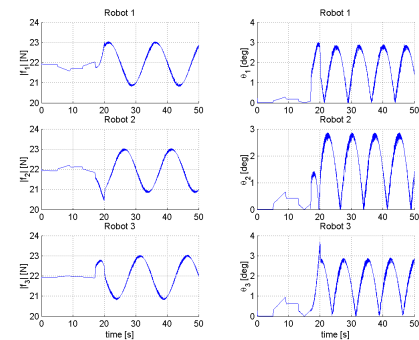


Fig. 9. Contact force trajectory while the load is tracking a circular trajectory

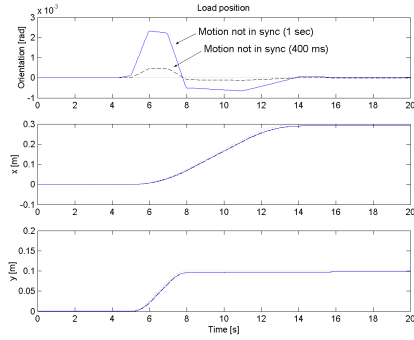


Fig. 10. Motion trajectory of load tracking a trapezoidal trajectory with the desired motion trajectory of robot 1 occurring 400ms and 1s before the other robots.

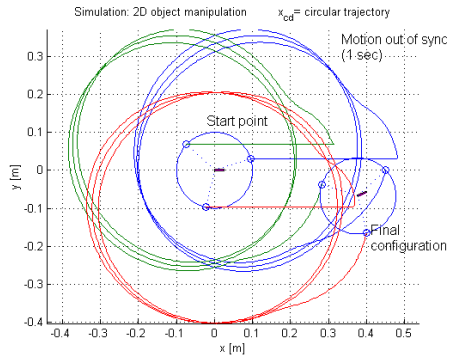


Fig. 11. Motion of load tracking a circular trajectory with the desired motion trajectory of robot 1 occurring 1s before the other robots.

#### Innovations (RTI).

During the experiments the robots are positioned to face each other and commanded to move a rigid, lightweight box horizontally, as shown in Figure 13. As the robot wrists are not perfectly aligned, we first need to estimate the squeeze subspace. We achieve this by applying infeasible setpoints to the decentralized motion controllers and recording the corresponding steady state position errors,  $\Delta x_k$ . The singular values of  $[\Delta x_1, \dots, \Delta x_k]$  are plotted in Fig. 15 versus the number of experiments. It can be seen that the squeeze subspace is one dimensional along the line connecting the two contact points (the other singular values are very small).

Then we moved the load along horizontal axis using the proposed decentralized motion and force control. As a first phase of the experiment, the position control is applied until the load is firmly grasped by the robots. The desired force is then set and the decentralized force control enabled. During the experiment the desired force setpoint is chosen to be 4N for the left arm and -4N for the right arm (along the squeeze direction determined above). After this phase we start to move the load along the desired trajectory. The experimental results of the position and force of both robots are presented in Figures 16 and 17. The force is well regulated while the robots are at rest. However, significant force error is present during the motion of the load and robots. This transient error is in part the consequence of

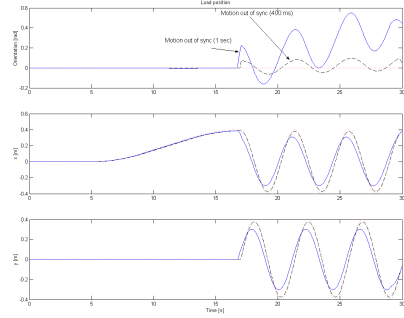


Fig. 12. Contact force trajectory while the load is tracking a circular trajectory with the desired motion trajectory of robot 1 occurring 400ms and 1s before the other robots.

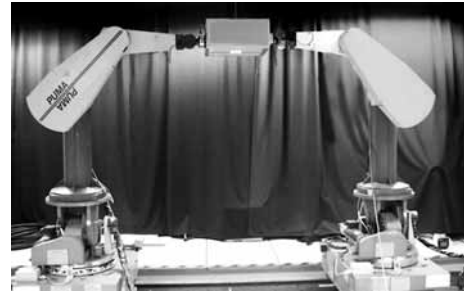


Fig. 13. Dual arm system

the asynchronous operation of the system in which each robot is commanded to start moving roughly at the same time, but they are not strictly synchronized.

#### V. CONCLUSIONS

This paper has presented the stability result of a fully decentralized motion and force control law for multiple robots rigidly grasping a load. In contrast to the common leader follower approach, all robots participate in both the motion and force control, allowing tighter regulation of force and higher motion speed. We are currently investigating the frictional contact case and conducting further experimental trials and tuning.

#### ACKNOWLEDGMENT

The authors would like to thank Real Time Innovations for the donation of Network Data Delivery Service software system used in the two-arm experimental testbed. Gustavo Montemayor is supported in part by CONACyT (Reg.132713), Mexico. This work is also supported in part by the National Science Foundation under Grant IIS-9820709 and the Center for Automation Technologies under a block grant from the New York State Office of Science, Technology, and Academic Research (NSTAR). This work is also supported in part by the China NSFC two-bases project under grant no. 60440420130.

#### REFERENCES

- [1] B. Hölldobler and E. Wilson, *The Ants*. The Belknap Press of Harvard University Press, 1990.



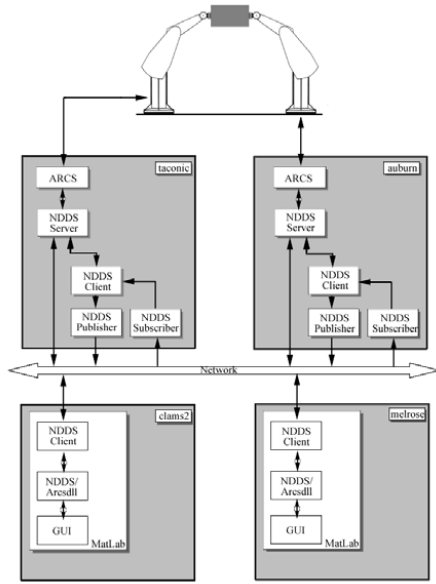


Fig. 14. Experimental setting

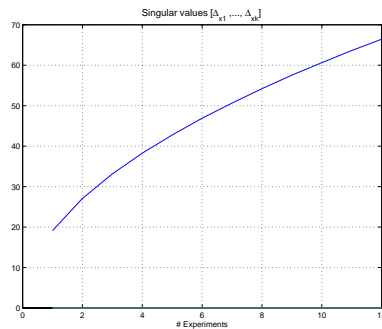


Fig. 15. Evolution of the singular values of  $[\Delta_{x_1}, \dots, \Delta_{x_k}]$

- [2] D. Stilwell and J. Bay, "Toward the development of a material transport system using swarms of ant-like robots," in *Proc. IEEE Int. Conf. Robotics and Automation*, 1993, pp. 766–771.
- [3] C. Kube and E. Bonabeau, "Cooperative transport by ants and robots," *Robotics and Autonomous Systems*, vol. 30, no. 1/2, pp. 85–101, 2000.
- [4] J. Wen and K. Kreutz-Delgado, "Motion and force control of multiple robotic manipulators," *Automatica*, vol. 28, no. 4, pp. 729–743, 1992.
- [5] K. Munawar and M. Uchiyama, "Experimental verification of distributed event-based control of multiple unfunctional manipulators," in *Proc. IEEE Int. Conf. Robotics and Automation*, May 1999, pp. 1213–1218.
- [6] M. Zribi and S. Ahmed, "Predictive adaptive control of multiple robots in cooperation motion," in *Proc. 30th IEEE Conf. Decision and Control*, Dec. 1991, pp. 2416–2421.
- [7] M. Koga, K. Kosuge, K. Furuta, and K. Nosaki, "Coordinated motion control of robot arms based in virtual internal model," *IEEE Trans. Robot. Automat.*, vol. 8, no. 1, pp. 77–85, 1992.
- [8] B. Yao and M. Tomizuka, "Adaptive coordinated control of multiple manipulators handling a constrained object," in *Proc. IEEE Int. Conf. Robotics and Automation*, 1993, pp. 344–349.
- [9] P. Pagilla and M. Tomizuka, "Adaptive control of two robot arms carrying an unknown object," in *Proc. IEEE Int. Conf. Robotics and Automation*, 1995, pp. 597–602.
- [10] T. Sugar, J. Desai, J. Ostrowski, and V. Kumar, "Coordination of multiple mobile manipulators," in *Proc. IEEE Int. Conf. Robotics and Automation*, 2001, pp. 3284–3289.

- [11] T. Sugar and V. Kumar, "Decentralized control of cooperating

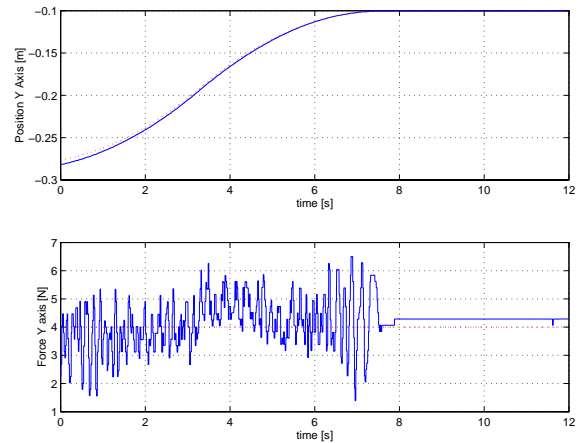


Fig. 16. Experimental results for the decentralized force control. Left PUMA

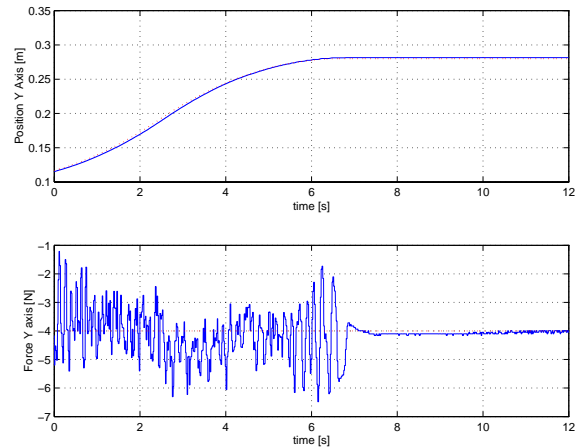


Fig. 17. Experimental results for the decentralized force control. Right PUMA

- mobile manipulators," in *Proc. IEEE Int. Conf. Robotics and Automation*, 1998, pp. 2916–2921.
- [12] L. Chaimowicz, T. Sugar, V. Kumar, and M. Campos, "An architecture for tightly couple multi-robot cooperation," in *Proc. IEEE Int. Conf. Robotics and Automation*, May 2001, pp. 2992–2997.
- [13] Y. Zheng and J. Luh, "Control of two coordinated robots in motion," in *Proc. 25th IEEE Conference on Decision and Control*, Ft. Lauderdale, FL, Dec. 1985, pp. 334–337.
- [14] O. Khatib, K. Yokoi, K. Chang, D. Ruspini, R. Holmberg, and A. Casal, "Vehicle/arm coordination and multiple mobile manipulator decentralized cooperation," in *Proc. IEEE/RSJ Int. Conf. Intelligent Robots and Systems*, vol. 2, 1996, pp. 546–553.
- [15] Y. Kume, Y. Hirata, Z. Wang, and K. Kosuge, "Decentralized control of multiple mobile manipulators handling a single object in coordination," in *Proc. IEEE/RSJ Int. Conf. Intelligent Robots and Systems*, vol. 3, Oct. 2002, pp. 2758–2763.
- [16] Y. Hirata, Y. Kume, Z. Wang, and K. Kosuge, "Decentralized control of multiple mobile manipulators based on virtual 3-D caster motion for handling an object in cooperation with a human," in *Proc. IEEE Int. Conf. Robotics and Automation*, vol. 1, 2003, pp. 938–943.
- [17] J. T. Wen and G. Montemayor, "Stability analysis of decentralized motion and force control for multiple robots," submitted to the 2005 American Control Conference, Sept. 2004.
- [18] J. Wen and D. Bayard, "Simple robust control laws for robotic manipulators, part I: Non-adaptive case," in *JPL/NASA Telerobotics Workshop*, Jan. 1987.